Improved helicopter aeromechanical stability analysis using segmented constrained layer damping and hybrid optimization

Qiang Liu, Aditi Chattopadhyay

Qiang Liu, Aditi Chattopadhyay, "Improved helicopter aeromechanical stability analysis using segmented constrained layer damping and hybrid optimization," Proc. SPIE 3985, Smart Structures and Materials 2000: Smart Structures and Integrated Systems, (22 June 2000); doi: 10.1117/12.388875

SPIE.

Event: SPIE's 7th Annual International Symposium on Smart Structures and Materials, 2000, Newport Beach, CA, United States

Improved helicopter aeromechanical stability analysis using segmented constrained layer damping and hybrid optimization

Qiang Liu† and Aditi Chattopadhyay*

Department of Mechanical and Aerospace Engineering
Arizona State University
Tempe, AZ 85287-6106

ABSTRACT

Aeromechanical stability plays a critical role in helicopter design and lead-lag damping is crucial to this design. In this paper, the use of segmented constrained damping layer (SCL) treatment and composite tailoring is investigated for improved rotor aeromechanical stability using formal optimization technique. The principal load-carrying member in the rotor blade is represented by a composite box beam, of arbitrary thickness, with surface bonded SCLs. A comprehensive theory is used to model the smart box beam. A ground resonance analysis model and an air resonance analysis model are implemented in the rotor blade built around the composite box beam with SCLs. The Pitt-Peters dynamic inflow model is used in air resonance analysis under hover condition. A hybrid optimization technique is used to investigate the optimum design of the composite box beam with surface bonded SCLs for improved damping characteristics. Parameters such as stacking sequence of the composite laminates and placement of SCLs are used as design variables. Detailed numerical studies are presented for aeromechanical stability analysis. It is shown that optimum blade design yields significant increase in rotor lead-lag regressive modal damping compared to the initial system.

1. INTRODUCTION

Aeromechanical stability of helicopters is a nonlinear phenomenon involving complex interactions between aerodynamic, inertial and elastic forces. Current advanced rotor designs tend towards hingeless and bearingless soft-inplane rotors. These rotor systems are susceptible to instabilities such as air and ground resonance due to the interaction of the poorly damped regressing lag mode and the body mode. Increase of lead-lag damping in rotor blades therefore is a crucial issue in an aeromechanical stability design. Recent research has shown that improvements in helicopter vibration reduction, aeroelastic stability and aeromechanical stability can be achieved by using smart materials and active control techniques. Elastomeric dampers have received significant amount of attention[1] due to the variety of advantages they exhibit over conventional dampers. However, these dampers are sensitive to temperature, exhibiting significant loss of damping at extreme temperatures and have been known to cause limit cycle oscillations in rotor blades. A numerical study of electrorheological (ER) dampers is presented in Re. 1. The feasibility of using Mgnetorheological fluid-based dampers for lag damping augmentation in helicopters is explored in Ref. 2. More recently, an enhanced active constrained damping layer (EACL) was developed for years for improvement of structural damping by Wang et al..[3,4] The use of segmented active constrained layer (ACL) damping treatment for active and passive augmentation of ground and air resonance stability was investigated by Badre et al. and Chattopadhyay et al..[5,6] The study indicates that significant improvement in lead-lag damping can be achieved through the use of this type of damping treatment.

The concept of active constrained layer (ACL) damping treatment was first proposed by Baz and Ro.[7-9] An active constrained damping layer (ACL) configuration comprises a piezoelectric layer and a viscoelastic bonding layer that connects the piezoelectric layer to the surface of the primary structure. The active constraining layer (piezoelectric layer) increases the shear deformation in the viscoelastic layer and therefore in reality forms an

---

† Graduate Research Associate, Member AIAA

* Professor, Associate Fellow AIAA, Member ASME, AHS, ISSMO

In *Smart Structures and Materials 2000: Smart Structures and Integrated Systems*, Norman M. Wereley, Editor, Proceedings of SPIE Vol. 3985 (2000) • 0277-786X/00/$15.00

effective means of enhancing the damping mechanism. Considerable amount of research has been performed in modeling ACLs, as summarized by Baz and Ro[7-9]. It is well known that segmented constraining layer is an effective means of increasing passive damping in low frequency vibration modes by increasing the number of high shear regions. A more comprehensive and practical approach to model sparse sequenced constrained layer (SCL) damping treatment on composite plates of arbitrary thickness was recently developed by Chattopadhyay et al.[10] In this work, a hybrid displacement theory was developed to efficiently model the transverse shear stresses in the various layers. Since the SCL configuration capitalizes on both passive and active damping techniques in a synergistic manner, it has been shown an effective method for vibration suppression in composite structures. In Ref. 5, a new form of ACL with edge element, known as EACL, was used in the flex beam of helicopter rotor blade to improve aeromechanical stability. In Ref. 6, the segmented SCL configuration was used to investigate improvement in passive inplane damping in rotor blade. The objective of this paper is to use optimization technique to address the complex design problems.

In this paper, a formal design optimization technique is used to investigate the optimum design of composite box beam with segmented constrained layers. A hybrid optimization algorithm,[11] which effectively incorporates continuous and discrete design variables using both gradient-based and discrete search strategies, is used for the design of the smart rotor blade with SCLs for maximizing the passive damping. The rotor blade load-carrying member is modeled using a composite box beam with arbitrary wall thickness. SCLs are surface bonded to the upper and lower horizontal surfaces of the box beam to provide passive damping. A hybrid displacement theory[10] is used to develop the governing equation of motion. A two-dimensional equivalent ground resonance model and an air resonance model are used to investigate the coupled rotor-body stability. The Pitt-Peters dynamic inflow model is used in the air resonance analysis under hover condition.[12] Parameters such as ply orientations and SCL placement are selected as discrete design variables. Constrains are imposed on the fundamental lead-lag and flap frequencies to ensure that the dynamic characteristics of the hingeless rotor are maintained.

2. STRUCTURAL MODELING

A composite box beam model of arbitrary wall thickness is used to represent the principal rotor load-carrying member in the rotor blade. SCLs are surface bonded to the top and bottom surfaces of the box beam (Fig. 1). Since an SCL consists of a piezoelectric layer and a viscoelastic bonding layer, it is necessary to accurately model the displacement fields, the boundary and the continuity conditions between the different layers. A new hybrid displacement theory was recently developed by Chattopadhyay et al.[10] to model surface bonded SCLs on a composite plate. The theory uses a higher order displacement field to capture the significant transverse shear effects in the composite primary structure. Since viscoelastic and piezoelectric layers are made from isotropic material, the first and the second order displacement fields are employed in these layers to maintain computational efficiency. The refined displacement fields, defined in the three different material layers, are derived by applying the displacement and transverse shear stress continuity conditions at the layer interfaces, and the traction-free boundary conditions on the top and the bottom surfaces of the structure. This plate model is then extended to develop a finite element model for the analysis of the composite box beam with surface bonded SCL damping treatment.[6] Details of this theory can be found in Ref. 6. A brief description of the model is presented below for the sake of completeness.

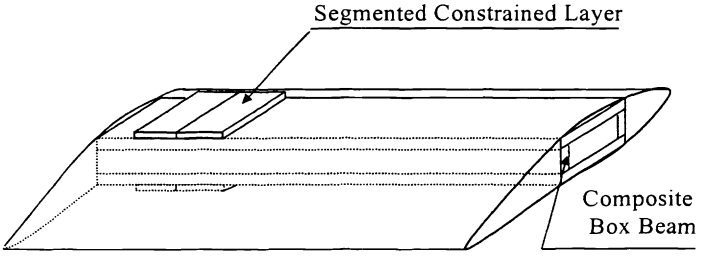

Fig. 1 Configuration of composite box beam with SCLs

The box beam is modeled using composite laminates representing the four walls (Fig. 2). In the hybrid displacement theory, each wall of the box beam is separated through the thickness into three different regions; composite region (region c), viscoelastic region (region v) and piezoelectric region (region p). The following refined displacement field is obtained after satisfaction of the boundary conditions.

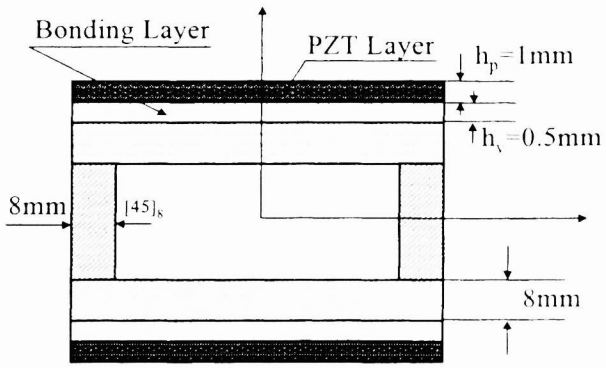

Fig. 2 Illustration of box beam element and walls with SCLs

$$
\begin{aligned}
u^c &= u_0^c - zw_{0,x}^c + z\left(1-\frac{4z^2}{3h^2}\right)\psi_x^c + \frac{2z^2}{3h^2}\left(z+\frac{3}{4}h\right)\frac{G^v}{G_{13}^c}\psi_x^v \\
v^c &= v_0^c - zw_{0,y}^c + z\left(1-\frac{4z^2}{3h^2}\right)\psi_y^c + \frac{2z^2}{3h^2}\left(z+\frac{3}{4}h\right)\frac{G^v}{G_{23}^c}\psi_y^v \qquad (1a)\\
w^c &= w_0^c \quad \text{where} -\frac{h}{2} \le z \le \frac{h}{2}
\end{aligned}
$$

$$
\begin{aligned}
u^v &= u_0^c + \frac{h}{3}\psi_x^c - zw_{0,x}^c + \left(z-\frac{h}{2}+\frac{5h}{24}\frac{G^v}{G_{13}^c}\right)\psi_x^v \\
v^v &= v_0^c + \frac{h}{3}\psi_y^c - zw_{0,y}^c + \left(z-\frac{h}{2}+\frac{5h}{24}\frac{G^v}{G_{23}^c}\right)\psi_y^v \qquad (1b)\\
w^v &= w_0^c \quad \text{where} \quad \frac{h}{2} \le z \le \frac{h}{2}+h_v
\end{aligned}
$$

$$
\begin{aligned}
u^p &= u_0^c + \frac{h}{3}\psi_x^c - zw_{0,x}^c + \left[\frac{G^v}{G^p}\frac{1}{2h_p}\left(2h_4 z - z^2 - h_3h_4 - h_3h_p\right) + h_v + \frac{5h}{24}\frac{G^v}{G_{13}^c}\right]\psi_x^v \\
v^p &= v_0^c + \frac{h}{3}\psi_y^c - zw_{0,y}^c + \left[\frac{G^v}{G^p}\frac{1}{2h_p}\left(2h_4 z - z^2 - h_3h_4 - h_3h_p\right) + h_v + \frac{5h}{24}\frac{G^v}{G_{23}^c}\right]\psi_y^v \qquad (1c)\\
w^p &= w_0^c \qquad \text{where} \quad \frac{h}{2}+h_v \le z \le \frac{h}{2}+h_v+h_p
\end{aligned}
$$

with

$$
h_3 = \frac{h}{2}+h_v, \qquad h_4 = \frac{h}{2}+h_v+h_p \qquad (2)
$$

where, u, v and w are the inplane and the out of plane displacements at a point (x,y,z), u_0, v_0 and w_0 represent the displacements at the midplane, ψ_x and ψ_y represent the rotations of the normals to the midplane. The quantity G is the shear modulus of the material. The present approach is able to capture the varying behaviors in the different material regions.

The continuity conditions at section interface require that the displacements defined in adjacent section (Eq. (1)) equal to each other through the thickness. These lead to the following

$$\psi_x^v(x,y) = \psi_y^v(x,y) = 0, \quad (x,y) \in \Gamma_s \tag{3}$$

where, Γ_s represents the section interface.

For the wall with segmented viscoelastic layer and piezoelectric constraining layer, the anelastic displacement field method is used to implement the viscoelastic material model. This enables time domain finite element analysis. For the wall with SCLs, the total displacement vector (u) is divided into two parts, the discretized displacement vector (u_g) which represents the wall displacement including the composite, the viscoelastic and the piezoelectric layers, and the anelastic displacement vector (u_v) pertaining to the viscoelastic layer.

$$u = \begin{Bmatrix} u_g \\ u_v \end{Bmatrix} \tag{4}$$

Using Hamilton's principle, the final governing equations of the box beam are expressed as follows.

$$M_g \ddot{u}_g + K_g u_g - K_{gv} u_v = F_g \tag{5}$$

where M_g and K_g are the structural global mass and stiffness matrices, respectively and K_{gv} is the additional structural global stiffness matrix due to the anelastic displacement vector (u_v). The quantity F_g is the external force.

An additional set of ordinary differential equation that describes the time evolution of the anelastic displacement field is employed to obtain the solution of the entire system.

$$\begin{bmatrix} M_g & 0 \\ 0 & 0 \end{bmatrix} \begin{Bmatrix} \ddot{u}_g \\ \ddot{u}_v \end{Bmatrix} + \begin{bmatrix} 0 & 0 \\ 0 & \frac{c}{\Omega_d} K_v \end{bmatrix} \begin{Bmatrix} \dot{u}_g \\ \dot{u}_v \end{Bmatrix} + \begin{bmatrix} K_g & -K_{gv} \\ -K_{gv}^T & cK_v \end{bmatrix} \begin{Bmatrix} u_g \\ u_v \end{Bmatrix} = \begin{Bmatrix} F_g \\ 0 \end{Bmatrix} \tag{6}$$

where K_v is the global stiffness matrix constituting anelastic strain, c is the material constitutive coupling parameter and Ω_d is the characteristic relaxation time at constant strain. The force boundary conditions are imposed to couple the box beam and viscoelastic bonding layer in time domain.

3. OPTIMIZATION METHOD

The optimization problem is formulated with the objective of determining the best locations of the SCLs along the blade spans while taking advantage of composite tailoring to improve rotor blade inplane damping. The hybrid optimization technique, developed by Chattopadhyay and Seeley,[11] is used in present study.

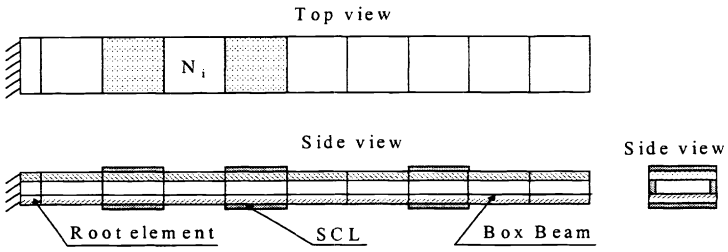

Fig. 3 Composite box beam configuration

Each pair of SCLs is located on the top and bottom surfaces of the box beam (Fig.3). The box beam is discretized using 11 elements (including the root element to adjust the root stiffness). The length and width of each SCL are the same as those of each element. This means the size of SCL is considered fixed and it entirely covers the surface of each element to which it is bonded.

The objective is to maximize first modal damping ratio (lead-lag damping), which can be stated as,

$$\eta_l = \frac{\mathrm{Re}(\lambda_1)}{\sqrt{\mathrm{Re}(\lambda_1)^2 + \mathrm{Im}(\lambda_1)^2}} \tag{7}$$

where λ_1 is the eigenvalue of the fundamental mode of the box beam, η_1 is the damping ratio corresponding to this mode.

The corresponding objective function is defined as follows

$$\text{Maximize} \quad f = -\eta_l \tag{8}$$

The box beam walls are assumed to comprise eight plies of equal thickness and the stacking sequence is assumed symmetric. Also the same ply stacking sequences are used for the top and bottom walls to reduce the number of design variables and the ply lay-ups are considered as discrete design variables θ_i (Eq.(9)). Therefore, a total of four variables are used to describe the stacking sequence of the top and bottom laminates, which are allowed to vary within a range of preselected ply orientations. Upper and lower bounds are imposed on these design variables to prevent large reductions in stiffness of the box beam in spanwise direction. Also the placement N_i of nth SCL pair is defined as a discrete variable based on the element number, on which the SCL is located. The upper and lower bounds of these variables are 1 and 10 (Since no SCLs are used on the root element). Therefore, the design variables are expressed as

$$\theta = [-\theta_1 / \theta_2 / -\theta_3 / \theta_4]_s \tag{9}$$

$$\begin{aligned} Y(i) &= \theta_i \quad (i = 1..4), 1 \le \theta_i \le 30 \\ X(i) &= N_i \quad (i = 1..3), 1 \le N_i \le 10 \end{aligned} \tag{10}$$

Three cases are studied in this research: one pair of SCLs (Case 1); two adjacent pairs of SCLs (Case 2); three pairs of SCLs (Case 3).

Constraints are imposed on the normalized fundamental lead-lag frequency ϖ_ξ and the normalized fundamental flap frequency ϖ_β of the box beam to ensure that the optimum blade design satisfies dynamic characteristics of a hingeless rotor. The constraints are defined as follows.

$$\begin{aligned} \varpi_\xi - 0.70 &\le 0 \\ 0.55 - \varpi_\xi &\le 0 \\ \varpi_\beta - 1.10 &\le 0 \end{aligned} \tag{11}$$

In the hybride theory, an exterior penalty method is used to incorporate the constraints as follows

$$F = F^c + \bar{\rho} \sum_{j=1}^{NCON} \max(0, g_j)^2 \tag{12}$$

where F^c is the objective function and $\bar{\rho}$ is a scalar penalty parameter, g_j represents the constraints and NCON is the total number of constraints.

4. GROUND AND AIR RESONANCE ANALYSIS

A classic ground resonance model is shown in Fig. 4a. In this model, only fundamental lead-lag mode is taken into account. Multiblade coordinates are used to transfer rotating coordinate into nonrotating coordinate. The fuselage is modeled as an equivalent mass, damper and spring system located at the hub center as shown in Fig. 4a. The lateral and longitudinal equivalent mass (M_{fx}, M_{fy}), stiffness (K_{fx}, K_{fy}) and damping (C_{fx} C_{fy}) represent the lateral and

longitudinal fuselage modal characteristics. The variable ξ_k is lead-lag displacement of the k-*th* blade. The lead-lag dynamic equation of the k-*th* blade can be expressed as

$$\ddot{\xi}_k + 2\eta\overline{\omega}_\xi\dot{\xi}_k + \overline{\omega}_\xi^2\xi_k + \frac{S_\xi}{I_\xi}(\ddot{\overline{X}}\sin\psi_k - \ddot{\overline{Y}}\cos\psi_k) = 0 \tag{13}$$

where ϖ_ξ is the lead-lag frequency ratio, ψ_k is the azimuth angle, S_ξ is the first mass moment and I_ξ is the blade lead-lag inertia. Quantities $\overline{X}$ and $\overline{Y}$ are dimensionless displacements of the hub center and η is the blade fundamental inplane critical modal damping ratio. This quantity (η) is obtained from the eigensolution of the box beam with segmented SCLs.

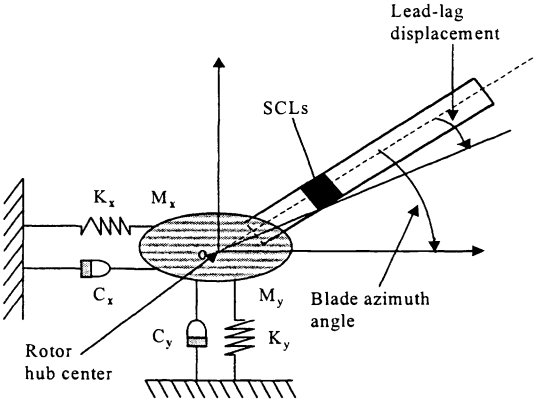

Fig. 4a Classical ground resonance model

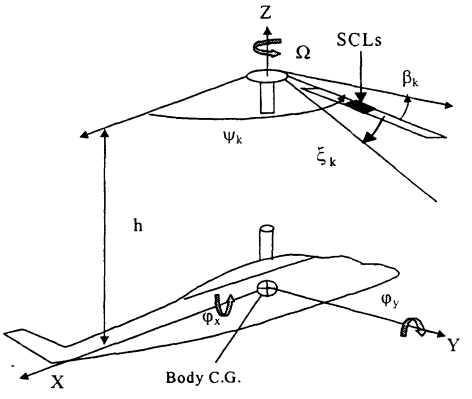

Fig. 4b Air resonance model

The air resonance model is shown in Fig. 4b. Only rigid body pitch and roll rotation degrees of freedom are taken into account in this model. A fundamental flap modal displacement (β_k) and a fundamental lead-lag modal displacement (ξ_k) are considered. It is also assumed that there is no geometric twist. The blade pitch degree of freedom is not included in the analysis. In Fig. 4b, variables φ_x and φ_y represent fuselage roll and pitch displacements, respectively. The center of gravity (C.G) of the helicopter is in the rotor shaft. The distance from the C.G. to the hub center is h. The variable ψ_k is the azimuth angle and Ω represents the rotor rotational speed. It is assumed that the blade mass is distributed uniformly along the blade span and the planform is assumed to be rectangular. To further simplify the problem, it is assumed that there is no structural coupling between flap and lead-lag motion. The individual blade flap and lead-lag motions are combined together and are transferred to the nonrotating coordinate through multiblade transformation. Similar to ground resonance analysis, the modal damping of the box beam with SCLs is calculated from Eq. 6 and is used in the blade flap and lead-lag equilibrium equations. In these equations, aerodynamic load is used as an external force vector acting on the rotor blade.

The aerodynamic forces are calculated based on quasi-steady lifting line theory, combined with a dynamic inflow model. This model, due to Pitt-Peters[12], can be expressed as follows.

$$v_1 = v_{1c}\bar{r}\cos\psi_k + v_{1s}\bar{r}\sin\psi_k \tag{14}$$

$$\begin{bmatrix} \frac{16}{45\pi} & 0 \\ 0 & \frac{16}{45\pi} \end{bmatrix}\begin{Bmatrix} v_{1s} \\ v_{1c} \end{Bmatrix} + \begin{bmatrix} v_s & 0 \\ 0 & v_s \end{bmatrix}\begin{Bmatrix} v_{1s} \\ v_{1c} \end{Bmatrix} = -\begin{Bmatrix} C_L \\ C_m \end{Bmatrix} \tag{15}$$

where v_1, v_{1c} and v_{1s} represent perturbations in the total, the cosine and the sine components of the induced velocity, respectively. The quantity $\bar{r}$ represents the blade radial station nondimensionalized with respect to rotor radius. The quantities v_s and ψ_k denote dimemsionless equilibrium velocity in hover and azimuth angle of k-*th* blade respectively and C_L and C_M are rolling and pitching moment coefficients, respectively.

The sectional lift (dF_z) and drag (dF_y) on the k-*th* blade can be written as follows.

$$\begin{aligned} dF_z &= \tfrac{1}{2}\rho ab(\theta U_T^2 - U_p U_T)dr \\ dF_y &= -\tfrac{1}{2}\rho ab(C_d U_T^2 - \theta U_p U_T - U_p^2)dr \end{aligned} \tag{16}$$

where a is the blade section lift-curve slope, b is the blade chord, θ is the collective pitch, and ρ is the air density. The quantities U_T and U_p are air velocities of blade section perpendicular and tangent to the disk plane, respectively. These can be expressed as follows.

$$\begin{aligned} U_T &= \Omega r - y' \\ U_p &= z' + v_0 + v_1 \Omega R \end{aligned} \tag{17}$$

where v_0 is the induced velocity of the helicopter in equilibrium hover condition and z' and y' are flap and lead-lag velocities, respectively.

5. RESULTS AND DISCUSSION

The aeromechanical behavior of a rotor blade built around the composite box beam, with top and bottom surface bonded SCLs, is studied in detail. The dimensions of the box beam (Fig.3) are such that length L=5.5*m*, width a=0.176*m* and high b=0.06*m*. Each wall comprises of eight layers with thickness t=1mm. The piezoelectric layer thickness (h_p) is 1mm. The viscoelastic layer thickness (h_v) is 0.5mm. Each SCL has the same width as that of the box beam. The box beam is discretized using 11 elements. The length of each SCL is the same as that of each element. The properties of the box beam are listed in Table 1.

Optimization is performed using the three different SCLs arrangements. The cases studied are described as:

Case1: one pair of SCLs move along the blade span;

Case2: two adjacent pairs of SCLs move along the blade span;

Case3: three pairs of SCLs move along the blade span.

Results for all cases are summarized in Table 2. As shown in Table 2, the fundamental lead-lag modal damping of the box beam is significantly increased in the optimal configurations, compared to the initial, for all three cases. The stacking sequence in the composite laminates tends to move towards upper bounds on the ply angles in an effort to improve extension-shear coupling. For all three cases studied, the initial placements (2; 2-3; 2-3-4) of the SCLs are closer to the root of the box beam, however, in the optimal configurations, they are closer to mid span. This is due to the fact that maximum extension-shear coupling occurs in blade mid span. The results also imply that the best locations of SCLs correspond to the region of largest inplane modal damping for all the three cases studied.

Results for the ground resonance model of the four bladed rotor are shown in Fig. 5. In this model, the ratio of blade first mass moment to blade inertia (S_ξ/I_ξ) is 1.5. The equivalent fuselage frequencies ω_x and ω_y are 7.94 and 5.58, respectively. The rotor normal angular velocity (Ω_0) is 37.5(1/s) and the fundamental lead-lag frequency ratio of the rotor blade, ϖ_ξ=0.62.

Table 1: Material properties of PZT and graphite/epoxy composite

	PZT	Viscoelastic layer	Graphite/Epoxy
E_{11}(GPa)	63	25	144.23
E_{22}(GPa)	63	25	9.65
E_{33}(GPa)	63	25	9.65
G_{23}(GPa)	24.6	10	3.45
G_{13}(GPa)	24.6	10	4.14
G_{12}(GPa)	24.6	10	4.14
ν_{12}	0.28	0.25	0.3
ν_{23}	0.28	0.25	0.3
ν_{31}	0.28	0.25	0.02
Density (kg/m^3)	7600	1600	1389.23
Piezoelectric Constant(pm/V)	254		
VEM	Ω_d=20(rad/sec)	C=1.2	

Table 2: Results of optimization

Cases Number	Stacking sequence (initial)	Stacking sequence (optimum)	Placement of SCLs (initial)	Placement Of SCLs (optimum)	Lead-lag damping (initial)	Lead-lag damping (optimum)
1	$[-15/15/-15/15]_s$	$[-29/30/-28/30]_s$	2	5	0.0132	0.0281
2	$[-15/15/-15/15]_s$	$[-30/30/-29/30]_s$	2,3	4,5	0.0319	0.0610
3	$[-15/15/-15/15]_s$	$[-28/30/-29/30]_s$	2,3,4	4,5,6	0.0481	0.0862

In Fig. 5, the variation of the ground resonance modal damping with rotor rotational speed is presented for two reference cases (reference 1: no SCL, no fuselage damping; reference 2: no SCL, with 20 percent fuselage damping) and both initial and optimal systems. The purpose of this comparison is to illustrate the effect of using SCLs which renders the initial unstable systems (references 1 and 2) to a stable system. The LR mode is unstable in both the reference cases with no SCL. However with one pairs of SCLs, the rotor-body coupled system becomes stable with LR modal damping of about 0.01 for the initial design (Case 1) and with further increase in Case 1 after optimization. Also with optimization, the LR modal damping increases significantly for Cases 2 after optimization. In Case 1, the LR modal damping is almost doubled with optimal design variables compared to the initial system. An increase of 25 percent LR modal damping is observed in Case 2 after optimization.

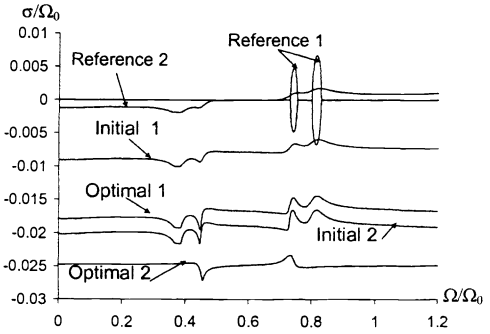

Fig. 5 Variation of ground resonance LR modal damping

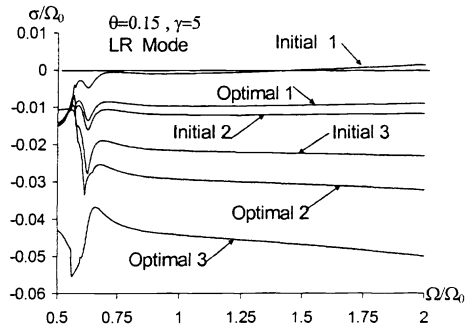

Fig. 6 Variation of air resonance LR modal damping

In the air resonance model, the ratio of blade first mass moment to blade inertia (S_ξ/I_ξ) is 1.5. The dimensionless fuselage roll and pitch inertia are 2.86 and 9.42, respectively. The rotor normal angular velocity (Ω_0) is 37.5(1/s). The fundamental flap and lead-lag frequency ratios of the rotor blade are ϖ_β=1.08 and ϖ_ξ=0.62, respectively. The blade airfoil profile lift-curve slop is 2π and the blade airfoil drag coefficient is 0.01. The dimensionless distance from the fuselage center of gravity to the rotor plane (h/R) is 0.312. In the system studied, a total of seven system modes are included: lead-lag regressive mode (LR), lead-lag advancing mode (LA), flap regressive mode (FR), flap advancing mode (FA), gyroscopic mode (GS), dynamic inflow mode (DI) and zero root mode.

In Fig. 6, the LR modal damping of air resonance with rotor rotational speed is shown. The results are computed for lock number γ=5 and collective pitch θ=0.15. As shown in Fig. 6, the LR mode of initial system (Initial 1) with one pair of SCL (Case 1) is unstable. With the application of optimization, the coupled rotor-body system is stabilized (Optimal 1). A modal damping of 0.01 for the LR mode is obtained over the entire rotor rotational speed. The lead-lag damping of the optimal designs in Cases 2 and 3 where two pairs and three pairs of SCLs, are used, is also much larger as shown in Fig. 6. The significant increase in lead-lag damping in optimal designs corresponding to Cases 2 and 3 are a result of increased high shear regions due to multiple SCLs.

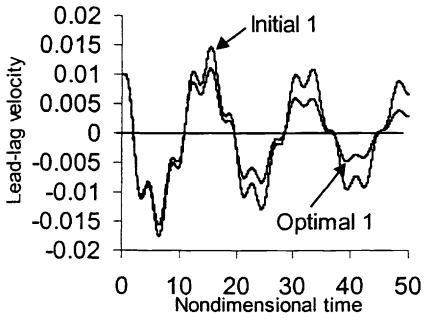

Fig. 7 Lead -lag response of initial and optimal systems (with one pair of SCLs)

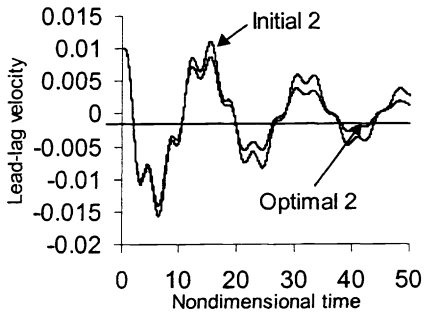

Fig. 8 Lead -lag response of initial and optimal systems (two pairs of SCLs)

Figures 7 and 8 show the time histories of cyclic lead-lag velocity response in air resonance analysis when two same initial velocities are exerted on the two cyclic lead-lag degrees of freedom in Cases 1 and 2. For the cases studied, the rotor operates at the normal angular velocity Ω_0. The frequencies of the system are 0.36 (LR), 1.74 (LA), 0.21 (FR), 1.84 (FA) and 0.06 (GS). The others are zero modes. It is observed that the convergence of two cyclic lead-lag responses in the optimal design is faster compared to the initial design due to increased lead-lag damping in the optimal system. The lead-lag advancing mode responses damp out within approximately 50 nondimensional time

(Ω_0t, about 1.3s in real time scale). It is obvious that LR mode decays at a much slower rate compared to LA mode. Also it can be observed that optimum design with two pairs of SCLs converge faster than that with one pair of SCLs.

6. CONCLUDING REMARKS

The use of a formal optimization strategy is investigated for improving passive lead-lag damping in rotor blade using segmented constrained layer damping. A hybrid optimization technique is used to address the complex design problem. The impact of passive damping on helicopter aeromechanical stability analysis, including ground and air resonance is investigated. A linear dynamic inflow model is used in the air resonance analysis under hover condition. The principal load-carrying member in the rotor blade is represented by a composite box beam with segmented constrained layers bonded on the top and bottom surfaces of the beam. A finite element model is developed for the analysis of the box beam using hybrid displacement field theory. The following important observations are made from the current study.

(1) Significant improvement in inplane fundamental modal damping is obtained using the hybrid optimization technique

(2) Optimum placements of SCLs are closer to mid span of the box beam where maximum extension-shear coupling occurs.

(3) Stacking sequence of the laminates are also driven by extension-shear coupling.

(4) The lead-lag regressive and lead-lag advancing modal responses of optimum systems decay at much faster rate compared to the initial systems.

ACKNOWLEDGMENT

The research was supported by the U.S. Army Research Office, grant number DAAH04-96-1-0163, technical monitor Dr. Gary Anderson.

REFERENCES

1. McGuire, D.P., "Fluidlastic® Dampers and Isolators for Vibration Control in Helicopters," Proc. American Helicopter Society 50th Annual Forum, Washington D.C., 1994. 295-303.

2. Kamath, G.M. and Wereley N.M., "Development of ER-Fluid Based Actuators for Rotorcraft Flexbeam Applications," *Proc. SPIE*, Vol. 2443, 120-133, 1995.

3. Liao, W.H., and Wang, K.W., "Characteristics of Enchanced Active Constrained Layer Damping Treatments with Edge Elements, Part 1: Finite Element Model development and Validation", Journal of Vibration and Acoustics-Transactions of the ASME, **120:(4)**, Oct. 1998, pp.886-893.

4. Liao, W.H., and Wang, K.W., "Characteristics of Enchanced Active Constrained Layer Damping Treatments with Edge Elements, Part 2: System Analysis", Journal of Vibration and Acoustics-Transactions of the ASME, **120:(4)**, Oct. 1998, pp.894-900.

5. Badre-Alam A., Wang K.W. and Gandhi F.,"Optimization of Enhanced Active Constrained Layer (EACL) Treatment on Helicopter Flexbeam for Aeromechanical stability Augmentation". *Smart Material structure*, 8 (1999), pp182-196.

6. Liu Q., Chattopadhyay, A., Gu, H. and Xu Zhou, "Effect of Active Constrained Damping Treatment on Helicopter Aeromechanical Stability Analysis" *55th AHS Annual Forum*, Montreal, Canada, May 25-27, 1999.

7. Baz, A. and Ro, J., "Partial Treatment of Flexible Beams with Active Constrained Damping," *Conf. of the Society of Engineering Science (ASME-AMD)*, Charlottesville, VA, Vol.167, 1993, 61-68.

8. Ro, J. and Baz, A., "Optimum Design and Control of Active Constrained Layer Damping," *Journal of Mechanical Design* and *Journal of Vibration and Acoustics* (special combined edition), 117(1996), 135-144.

9. Baz, A. and Ro, J., "Finite Element Modeling and Performance of Active Constrained Layer Damping," *Proc. of 9th VPI&SU Conf. dynamics and control of large Structures*, Blacksburg, VA, 345-358.

10. Haozhong Gu, Aditi Chattopadhyay and Changho Nam, "Modeling Segmented Active Constrained Layer Damping Using Hybrid Displacement Field," *AIAA 99-1542.*

11. Chattopadhyay A., Seeley, C.E. and Jha, R., "Aeroelastic Tailoring Using Piezoelectric Actuation and Hybrid Optimization", *Smart Materials & Materials*, 8, 1999, pp.83-91.

12. Pitt, D.M., Peters, D.A., " Theoretical Predictions of Dynamic Inflow Derivatives", Vertica, Vol. 5, No.1, March 1981.